

Comparative Study on Maxwell and Navier Stokes Fluid Equations with Pressure Gradient Over a Flat Plate for Convective Boundary Layer Flow and Heat Transfer

¹Amber Nehan Kashif* and ²Zainal Abdul Aziz

^{1,2}Department of Mathematical Sciences, Faculty of Science
81310 UTM, Johor Bahru, Johor, Malaysia

¹Department of Mathematical Sciences, Faculty of Science, FUUAST, Karachi, Pakistan

²UTM Centre for Industrial and Applied Mathematics.
Institute of Scientific and Industrial Research, UTM
81310 UTM, Johor Bahru, Johor, Malaysia

*Corresponding author: ankashif@gmail.com

Article history

Received: 2 August 2017

Received in revised form: 12 November 2017

Accepted: 23 November 2017

Published on line: 1 June 2018

Abstract In this paper, Maxwell fluid over a flat plate for convective boundary layer flow with pressure gradient parameter is considered. The aim of this study is to compare and analyze the effects of the presence and absence of λ (relaxation time), and also the effects of m (pressure gradient parameter) and Pr (Prandtl number) on the momentum and thermal boundary layer thicknesses. An approximation technique namely Homotopy Perturbation Method (HPM) has been used with an implementation of Adam and Gear Method's algorithms. The obtained results have been compared for zero relaxation time and also pressure gradient parameter with the published work of Fathizadeh and Rashidi. The current outcomes are found to be in good agreement with the published results. Physical interpretations have been given for the effects of the m , Pr and β (Deborah number) with λ . This study will play an important role in industrial and engineering applications.

Keywords Maxwell fluid equation; Navier-Stokes equations; pressure gradient; relaxation time; homotopy perturbation method (HPM); Adams method (AM); Gear method (GM).

Mathematics Subject Classification 46N60, 92B99.

1 Introduction

The flow of fluids in the geophysics, atmospheric sciences, oceanography, astrophysics, biological sciences and technologies etc., is effected by the pressure exerted by the various conditions, chemical compositions and forces on the fluid flow. The stress and rate of strain relationship explains the non-Newtonian fluids. The complexity, non-linearity and behaviour of non-Newtonian fluids for various applications have been discussed in Chhabra [1] and Málek [2].

The Maxwell fluid is simpler category of rate type non Newtonian fluids. It explores the effects of stress relaxation also it becomes the Naviera-Stokes, keeping extra stress time zero Hayat *et al.* [3], Noor [4] and Motsa *et al.* [5]. For the understanding of the dynamics of viscoelastic material, a continuous research have been conducted by James Clerk Maxwell in 1867 [6]. In an article “On the Dynamical Theory of Gases” Maxwell has discussed the equation of continuity, motion and system of pressures at any point of the fluid also the properties of elasticity and viscosity under the dynamics of materials [7]. Some other researchers have also discussed the flow of Maxwell fluid in Shateyi [8], Abbas *et al.* [9] and Hayat *et al.* [10]. Due to the growing industrial, engineering, chemical, scientific applications, cooling of electronic devices by fans, cooling of nuclear reactors during emergency shutdown and hydrodynamic processes the pressure gradient have got attention of engineers, chemists, scientists and researchers [11].

Pressure gradient is the point in the flow field where local velocity of the fluid becomes zero. The pressure gradient identifies the place in the fluid flow where the forthcoming flow splits to move on both boundaries along the surface. This flow exists all over the place in the sense that definitely appears as a part of more complex flow fields. Exemplarily in some situations, flow becomes stagnated due to a solid wall on the other hand there is a line interior to a homogeneous fluid domain or the interface between two immiscible fluids [12]. Bernoulli equation illustrates that the stagnation pressure is at maximum value when the fluid velocity is zero known to be the total pressure in terms of static pressure [13].

Homotopy Perturbation Method (HPM) has been taken as an approximation technique, many researchers like Ji-Huan and others have discussed it’s effectiveness and novelty in [14–17]. Later on this method has been further developed and improved by Ji-Huan and other researchers in [18–20]. To have solution of this problem, the two main algorithms, the Adams Method (AM) [21] and Gear Method (GM) [22] have been used in [23]. Now, this has become the case of the comparative study on Maxwell and Navier-Stokes fluid equations with pressure gradient over a flat plate for convective boundary layer flow and heat transfer. Here, HPM as an approximation technique has been implemented. The effect of pressure gradient m is studied for different Deborah Numbers β and Prandtl numbers Pr upon velocity and temperature profiles.

Present study with the inclusion of effects of pressure gradient will play an important role in many industrial and engineering applications those come across in extrusion development, like compulsive convection in conduits, paper and fibre glass production, paints application, electronic chips, material processing, crystal growth, nuclear reactor cooling, food processing and movement of biological fluids, drilling muds, shampoo, ketchup, cement, sludge, grease, granular suspension, aqueous foams, slurries, plastics and several others [24,25] and the references therein. To the best of our knowledge, this problem has not been studied before and the results reported here are new and original.

2 Basics of HPM

The fundamental concepts of this technique are given as follows:

Consider the nonlinear differential equation

$$A(u) - f(r) = 0, \quad r \in \Omega \quad (1)$$

Table 1: Nomenclature

Notation	
u, v	Fluctuating Velocity Components in x and y Directions
n	Number of Approximations
T	Temperature
T_w	Wall Temperature
T_∞	Local Ambient Temperature
H	Convective Heat Transfer Coefficient
P	Pressure
L	Linear Operator
N	Non-linear Operator
AM	Adams Method
GM	Gear Method
NM	Numerical Method
HPM	Homotopy Perturbation Method
f	Dimensionless Velocity Function
m	Pressure Gradient Parameter
Pr	Prandtl Number
p	Embedding Parameter of Homotopy
$q(r)$	Analytic Function
A	General Differential Operator
B	Boundary Operator
c_p	Specific Heat
x, y	Coordinates Along and Perpendicular to The Plate
Greek Symbols	
Γ	The Boundary of The Domain Ω
ρ	The Fluid Density
κ	The fluid thermal conductivity
μ	The coefficient of fluid viscosity
η	Dimensionless Variable
δ	Boundary Layer Thickness
ν	The Kinematics Fluid Viscosity
θ	Dimensionless Temperature
ψ	Streamline Function
β	Deborah Number
λ	The Relaxation Time or Maxwell Parameter

with boundary conditions

$$B(u, \partial u / \partial n) = 0, \quad r \in \Gamma \quad (2)$$

where A is a differential operator, B is an operator, $f(r)$ is an analytic function, Γ is the domain Ω boundary. A can be presented as a sum of L linear and N nonlinear, therefore, Eq.(1) is of the form:

$$L(u) + N(u) - f(r) = 0. \quad (3)$$

By the homotopy method [26] and [27], a homotopy $v(r, P) : \Omega \times [0, 1] \rightarrow R$ is constructed, which satisfies

$$\begin{aligned} H(v, p) &= (1 - p)[L(v) - L(u_o)] + p[A(v) - f(r)] = 0, \\ p &\in [0, 1], \quad r \in \Omega \end{aligned} \quad (4)$$

Or

$$H(v, p) = L(v) - L(u_o) + pL(u_o) + p[N(v) - f(r)] = 0, \quad (5)$$

where $p \in [0, 1]$ is a parameter which is embedded, u_0 is the initial approximated solution of Eq.(1), where the boundary conditions are fulfilled. Clearly, from Eq.(4 or 5) H takes the forms

$$H(v, 0) = L(v) - L(u_o) = 0, \quad (6)$$

$$H(v, 1) = A(v) - f(r) = 0, \quad (7)$$

the transformation of p from 0 to 1 is referred to $v(r, p)$ from $u_0(r)$ to $u(r)$. Topologically, this is known as deformation, besides $L(v) - L(u_0)$, $A(v) - f(r)$ are termed homotopic. In this study, the embedding parameter p as a small parameter and assumed that the solution of Eq.(4 or 5) can be written as a power series in p :

$$v = v_0 + pv_1 + p^2v_2 + \dots \quad (8)$$

Setting $p = 1$ results in the approximate solution of Eq.(1):

$$u = \lim_{p \rightarrow 1} v = v_0 + v_1 + v_2 + \dots \quad (9)$$

The coupling of the perturbation method and the homotopy method is called the homotopy perturbation method, which has eliminated limitations of the traditional perturbation methods. On the other hand, the proposed technique can take full advantage of the traditional perturbation techniques.

3 Mathematical Formulation

Consider the boundary layer flow over a flat plate having pressure gradient for Maxwell fluid is governed by the continuity and the momentum equations. The governing equations of continuity, motion and the energy may be written in usual notation as [25, 28, 29]:

$$\frac{\partial u}{\partial x} + \frac{\partial v}{\partial y} = 0 \quad (10)$$

$$u \frac{\partial u}{\partial x} + v \frac{\partial u}{\partial y} + \lambda \left[u^2 \frac{\partial^2 u}{\partial x^2} + v^2 \frac{\partial^2 u}{\partial y^2} + 2uv \frac{\partial^2 u}{\partial x \partial y} \right] = -\frac{1}{\rho} \frac{dP}{dx} + \nu \frac{\partial^2 u}{\partial y^2} \quad (11)$$

and

$$u \frac{\partial T}{\partial x} + v \frac{\partial T}{\partial y} = \frac{\kappa}{\rho c_p} \frac{\partial^2 T}{\partial y^2}, \quad (12)$$

subject to the boundary conditions:

$$\begin{aligned} u = 0, \quad v = 0, \quad T = T_w \quad \text{at} \quad y = 0, \\ u = U_\infty, \quad T \rightarrow T_\infty \quad \text{at} \quad y \rightarrow \infty, \end{aligned} \quad (13)$$

where u and v are the velocity components in x - and y - directions respectively, ν is the kinematic fluid viscosity, ρ is the fluid density, μ is the coefficient of fluid viscosity, λ is the relaxation time, T is the temperature, κ is the fluid thermal conductivity and c_p is the specific heat. Now, the stream function $\psi(x, y)$ is introduced as:

$$u = \frac{\partial \psi}{\partial y}, \quad v = -\frac{\partial \psi}{\partial x}. \quad (14)$$

For an external flow $-\frac{1}{\rho} \frac{dP}{dx}$ can be replaced by $U_\infty \frac{dU_\infty}{dx}$, where as in relations with equation (14), the equation (10) is identically satisfied and the equations (11 and 12) are reduced to the following forms:

$$\begin{aligned} \frac{\partial \psi}{\partial y} \frac{\partial^2 \psi}{\partial x \partial y} - \frac{\partial \psi}{\partial x} \frac{\partial^2 \psi}{\partial y^2} + \lambda \left[\left(\frac{\partial \psi}{\partial y} \right)^2 \frac{\partial^3 \psi}{\partial x^2 \partial y} + \left(\frac{\partial \psi}{\partial x} \right)^2 \frac{\partial^3 \psi}{\partial y^3} - 2 \frac{\partial \psi}{\partial y} \frac{\partial \psi}{\partial x} \frac{\partial^3 \psi}{\partial x \partial y^2} \right] \\ = U_\infty \frac{dU_\infty}{dx} + \nu \frac{\partial^3 \psi}{\partial y^3} \end{aligned} \quad (15)$$

and

$$\frac{\partial \psi}{\partial y} \frac{\partial T}{\partial x} - \frac{\partial \psi}{\partial x} \frac{\partial T}{\partial y} = \frac{\kappa}{\rho c_p} \frac{\partial^2 T}{\partial y^2}. \quad (16)$$

We introduce the dimensionless variables η , ψ and θ as:

$$\begin{aligned} \eta = y \sqrt{\frac{U_\infty}{\nu x}}, \quad \psi = f(\eta) \sqrt{\nu x U_\infty}, \quad \theta(\eta) = \frac{T - T_\infty}{T_w - T_\infty} \quad \text{and} \\ \left\{ U_\infty = bx^m, \quad m = \frac{x}{U_\infty} \frac{dU_\infty}{dx} \right\}, \end{aligned} \quad (17)$$

where T_w the temperature at wall, U_∞ the uniform free stream velocity. Based on equation (17), we have used similarity transformation to reduce the governing differential equations (15) and (16) to an ordinary non-linear differential equations (18) and (19) respectively.

$$\begin{aligned} f''' + m(1 - f'^2) + \left(\frac{m+1}{2} \right) f f'' - \frac{\beta}{2} [(m-1)(3-m)\eta f'^2 f'' + 4m(m+1)f'^3 \\ + (m+1)^2 f^2 f''' - 2(m+1)(3m-1) f f' f''] = 0, \end{aligned} \quad (18)$$

$$\theta'' + \frac{Pr(m+1)}{2} f \theta' = 0, \quad (19)$$

where $\beta = \lambda U_\infty(x)/2x$ is Deborah number [30] and $Pr = \mu c_p / \kappa$ is the Prandtl number [31]. The boundary conditions are obtained from the similarity variables,

$$\begin{aligned} f(0) = 0, \quad f'(0) = 0, \quad f'(\eta_\infty) = 1, \\ \theta(0) = 1, \quad \theta(\eta_\infty) = 0. \end{aligned} \quad (20)$$

4 HPM Solution

According to HPM method and equation (18) and (19) becomes:

$$\begin{aligned}
 & (1 - p)(f''' - f_0''') + p\left(f''' + \left(\frac{m + 1}{2}\right) f f'' + m(1 - f'^2)\right. \\
 & - \frac{\beta}{2}[(m - 1)(3 - m)\eta f'^2 f'' + 4m(m + 1)f'^3 + (m + 1)^2 f^2 f'' \\
 & \left. - 2(m + 1)(3m - 1) f f' f''\right]) = 0
 \end{aligned}
 \tag{21}$$

$$(1 - p)(\theta'' - \theta_0'') + p\left(\theta'' + \frac{Pr(m + 1)}{2} f \theta'\right) = 0
 \tag{22}$$

$$f = f_0 + p f_1 + p^2 f_2 + \dots,
 \tag{23}$$

$$\theta = \theta_0 + p \theta_1 + p^2 \theta_2 + \dots.
 \tag{24}$$

Assuming $f''' = 0$, $\theta'' = 0$, and substituting f from equation (23) into equation (21) and θ from equation (24) into equation (22) after some simplification and rearrangement based on powers of p -terms, we have:

$$\begin{aligned}
 p^0 : \quad & f_0''' = 0, \\
 & f_0(0) = 0, \quad f_0'(0) = 0, \quad f_0'(\eta_\infty) = 1, \\
 & \theta_0'' = 0, \\
 & \theta_0(0) = 1, \quad \theta_0(\eta_\infty) = 0
 \end{aligned}
 \tag{25}$$

$$\begin{aligned}
 p^1 : \quad & f_1''' = m(f_0'^2 - 1) - \left(\frac{m + 1}{2}\right) f_0 f_0'' + 2m(m + 1)\beta f_0^3 \\
 & + (1 - 2m - 3m^2)\beta f_0 f_0' f_0'' + \frac{1}{2}(4m - 3\eta - m^2\eta)\beta f_0'^2 f_0'', \\
 & f_1(0) = 0, \quad f_1'(0) = 1, \quad f_1'(\eta_\infty) = 0, \\
 & \theta_1'' = -\frac{Pr(m + 1)}{2} f_0 \theta_0', \\
 & \theta_1(0) = 0, \quad \theta_1(\eta_\infty) = 0
 \end{aligned}
 \tag{26}$$

$$\begin{aligned}
 p^2 : \quad & f_2''' = 2m f_0' f_1' - \left(\frac{m + 1}{2}\right) (f_1 f_0'' + f_0 f_1'') + 6\beta m(m + 1) f_0'^2 f_1' \\
 & + \beta(1 - 2m - 3m^2) \times (f_0' f_1 f_0'' + f_0 f_0' f_1'' + f_0 f_1' f_0'') \\
 & + \beta\eta(-3 + 4m - m^2) \left(f_0' f_1' f_0'' + \frac{1}{2} f_0'^2 f_1''\right) + \beta \frac{(m + 1)^2}{2} (f_0^2 f_1'''), \\
 & f_2(0) = 0, \quad f_2'(0) = 1, \quad f_2'(\eta_\infty) = 0, \\
 & \theta_2'' = -\frac{Pr(m + 1)}{2} (f_0 \theta_1' + f_1 \theta_0'), \\
 & \theta_2(0) = 0, \quad \theta_2(\eta_\infty) = 0
 \end{aligned}
 \tag{27}$$

$$\begin{aligned}
p^3 : \quad f_3''' &= m f_1'^2 + 2m f_0' f_2' - \left(\frac{m+1}{2} \right) \times (f_2 f_0'' + f_1 f_1'' + f_0 f_2'') + \\
&6\beta m(m+1) (f_0' f_1'^2 + f_0'^2 f_2') + \beta(1-2m-3m^2)(f_2 f_0' f_0'' + f_1 f_1' f_0'' + \\
&f_0 f_2' f_0'' + f_1 f_0' f_1'' + f_0 f_1' f_1'' + f_0 f_0' f_2'') + \beta\eta(-3+4m-m^2) \\
&\left(\frac{1}{2} f_1'^2 f_0'' + f_0' f_2' f_0'' + f_0' f_1' f_1'' + \frac{1}{2} f_0'^2 f_2'' \right) + \beta(1+2m+m^2) \\
&\left(f_0 f_1 f_1''' + \frac{1}{2} f_0'^2 f_2''' \right), \\
f_3(0) &= 0, \quad f_3'(0) = 1, \quad f_3'(\eta_\infty) = 0, \\
\theta_3'' &= -\frac{Pr(m+1)}{2} (f_0 \theta_2' + f_1 \theta_1' + f_2 \theta_0'), \\
\theta_3(0) &= 0, \quad \theta_3(\eta_\infty) = 0
\end{aligned} \tag{28}$$

Solving equations (25)-(28):

$$f_0 = \frac{1}{2\eta_\infty}(\eta^2) \tag{29}$$

$$\begin{aligned}
f_1 &= \frac{1}{480\eta_\infty^3} (-4\beta\eta^6 + 12\beta\eta^2\eta_\infty^4 - 2\eta^5\eta_\infty + 5\eta^2\eta_\infty^4 + 12\beta\eta^6 m - 36\beta\eta^2\eta_\infty^4 m \\
&+ 6\eta^5\eta_\infty m - 80\eta^3\eta_\infty^3 m + 105\eta^2\eta_\infty^4 m)
\end{aligned} \tag{30}$$

$$\begin{aligned}
f_2 &= \frac{1}{2419200\eta_\infty^5} (812\beta^2\eta^{10} - 3024\beta^2\eta^6\eta_\infty^4 + 5012\beta^2\eta^2\eta_\infty^8 + 800\beta\eta^9\eta_\infty \\
&- 1260\beta\eta^6\eta_\infty^4 - 1008\beta\eta^5\eta_\infty^5 + 2700\beta\eta^2\eta_\infty^8 + 165\eta^8\eta_\infty^2 \\
&- 420\eta^5\eta_\infty^5 + 390\eta^2\eta_\infty^8 - \dots)
\end{aligned} \tag{31}$$

$$\begin{aligned}
f_3 &= \frac{1}{83026944000\eta_\infty^7} (2067120m^5\beta^3\eta^{14} - 29150880m^4\beta^3\eta^{14} \\
&+ 88679360m^3\beta^3\eta^{14} - 60281760m^2\beta^3\eta^{14} + 15444880m\beta^3\eta^{14} \\
&- 1383360\beta^3\eta^{14} + 1134000m^5\beta^2\eta_\infty\eta^{13} - 18265680m^4\beta^2\eta_\infty\eta^{13} \\
&+ 61430880m^3\beta^2\eta_\infty\eta^{13} - \dots)
\end{aligned} \tag{32}$$

$$\theta_0 = \frac{1}{\eta_\infty}(-\eta + \eta_\infty) \tag{33}$$

$$\theta_1 = \frac{1}{48\eta_\infty^2} (\eta^4 m(Pr) - \eta\eta_\infty^3 m(Pr) + \eta^4(Pr) - \eta\eta_\infty^3(Pr)) \tag{34}$$

$$\begin{aligned}
\theta_2 &= \frac{1}{80640\eta_\infty^4} (-40\eta^7 m^2(Pr)^2\eta_\infty + 35\eta^4 m^2(Pr)^2\eta_\infty^4 + 5\eta m^2(Pr)^2\eta_\infty^7 \\
&+ 18\beta\eta^8 m^2(Pr) - 252\beta\eta^4 m^2(Pr)\eta_\infty^4 + 234\beta\eta m^2(Pr)\eta_\infty^7 + 12\eta^7 m^2(Pr)\eta_\infty \\
&- 336\eta^5 m^2(Pr)\eta_\infty^3 + 735\eta^4 m^2(Pr)\eta_\infty^4 - 411\eta m^2(Pr)\eta_\infty^7 \\
&- 80\eta^7 m(Pr)^2\eta_\infty + 70\eta^4 m(Pr)^2\eta_\infty^4 + \dots)
\end{aligned} \tag{35}$$

$$\begin{aligned}
\theta_3 = & \frac{1}{638668800\eta_\infty^6} (2772m^4(\text{Pr})\beta^2\eta^{12} + 1176m^3(\text{Pr})\beta^2\eta^{12} + 1232m^2(\text{Pr})\beta^2\eta^{12} \\
& + 1960m(\text{Pr})\beta^2\eta^{12} - 868(\text{Pr})\beta^2\eta^{12} - 8640m^3(\text{Pr})^2\beta\eta_\infty\eta^{11} \\
& - 14400m^2(\text{Pr})^2\beta\eta_\infty\eta^{11} - 2880m(\text{Pr})^2\beta\eta_\infty\eta^{11} \\
& + 2880(\text{Pr})^2\beta\eta_\infty\eta^{11} + 864m^4(\text{Pr})\beta\eta_\infty\eta^{11} + \dots)
\end{aligned} \tag{36}$$

5 Results and Discussions

The aim of this section is to analyze the effects of various physical parameters on the velocity and temperature distributions such as momentum and thermal boundary layer thicknesses. The validation of the present method using HPM is checked with the results obtained by Fathizadeh and Rashidi [32] and the numerical results reported in it for the Newtonian fluids, because Maxwell fluid equation becomes Navier-Stokes equation when Maxwell parameter λ the relaxation time is taken to zero (i.e $\lambda = 0$). The Deborah number β becomes 0 because $\beta \propto \lambda$ (i.e $\beta = 0$), Bhattacharyya *et al.* [25] reported that for Maxwell fluid $\beta > 0$. when Deborah number is taken as $\beta = 0$. So the numerical values in [32] can be compared in case of pressure gradient parameter $m = 0$. The reported results are the effects of m as well as β for the different values.

Figure 1 represents Velocity profile for $f'(\eta)$ for the different values of m when $\beta = 0$. Physically, Because of β zero it becomes the case of Newtonian fluid the results are same as in . The separation point flow is observed for lower value of $m = -0.120$ it means the fluid is not in contact with the surface. Where as, a two dimensional stagnation point flow is obtained at the higher value of $m = 0.00$ which prevents the development of the boundary layer growth. Higher value of m depicts the fluid flow is faster. It is observed that the velocity profile increases with increasing m consequently, the momentum boundary layer thickness becomes thicker and thicker.

Figure 2 is the pictorial comparison of the velocity profile $f'(\eta)$ for the value of $\beta = 0$ in Numerical, Navier-Stokes, Fathizadeh and Rashidi [32], also the Maxwell fluid results [32].

In Figure 3 represents $\theta(\eta)$ for the values m at $\beta = 0$ and $\text{Pr} = 1$. Physically, the separation point flow is observed for higher value of $m = 0.025$ it means the fluid is not in contact with the wall. Where as, a two dimensional stagnation point flow is obtained at the lower value of $m = -0.081$ which prevents the development of the boundary layer growth. Also show that the energy profile decreases with increasing m consequently, the momentum boundary layer becomes thinner and thinner.

Figure 4 is the pictorial comparison of the energy profile $f'(\eta)$ for the value of $\beta = 0$ and $\text{Pr} = 1$ in Numerical, Navier-Stokes, Fathizadeh and Rashidi [32], also the Maxwell fluid results [32].

Table 2 shows the data of the values of m when $\beta = 0$ from Figure 1. Table 3 shows the absolute error for $f'(\eta)$ of the different results. Table 4 shows the tabular values of $\theta(\eta)$ for the Figure 3. Table 5 shows the absolute error for $\theta(\eta)$ of the different results.

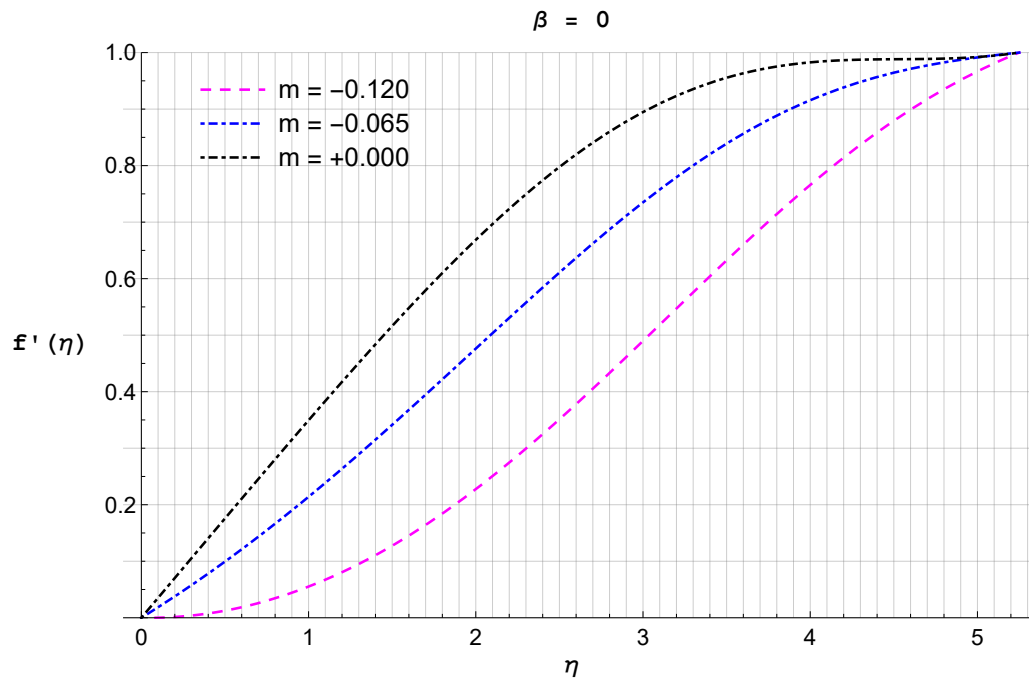


Figure 1: $f'(\eta)$ for the Values m When $\beta = 0$

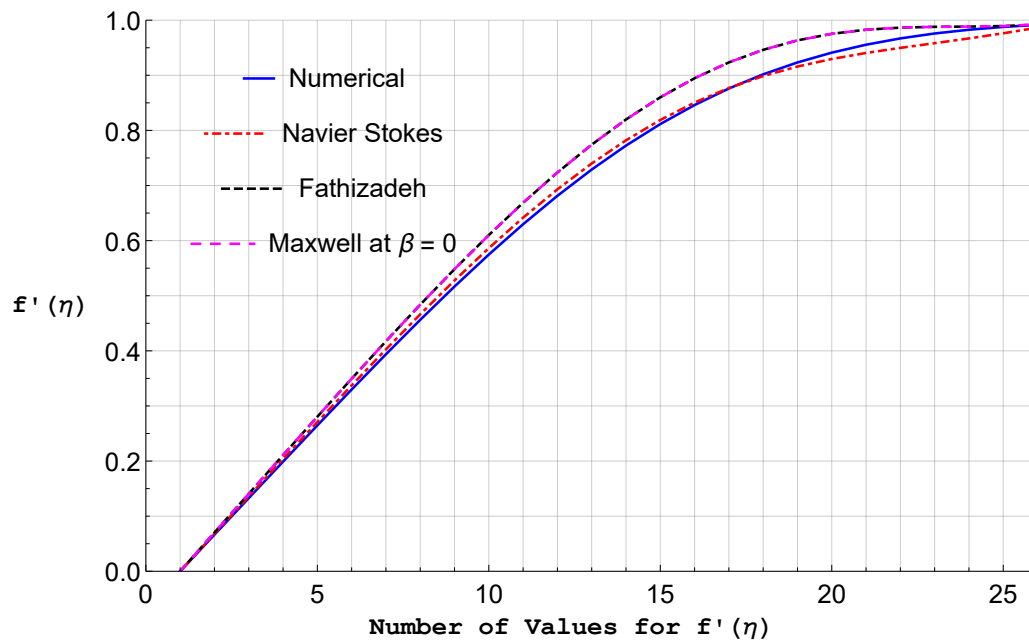


Figure 2: The Pictorial Comparison of $f'(\eta)$ for the Values $m = 0$ When $\beta = 0$

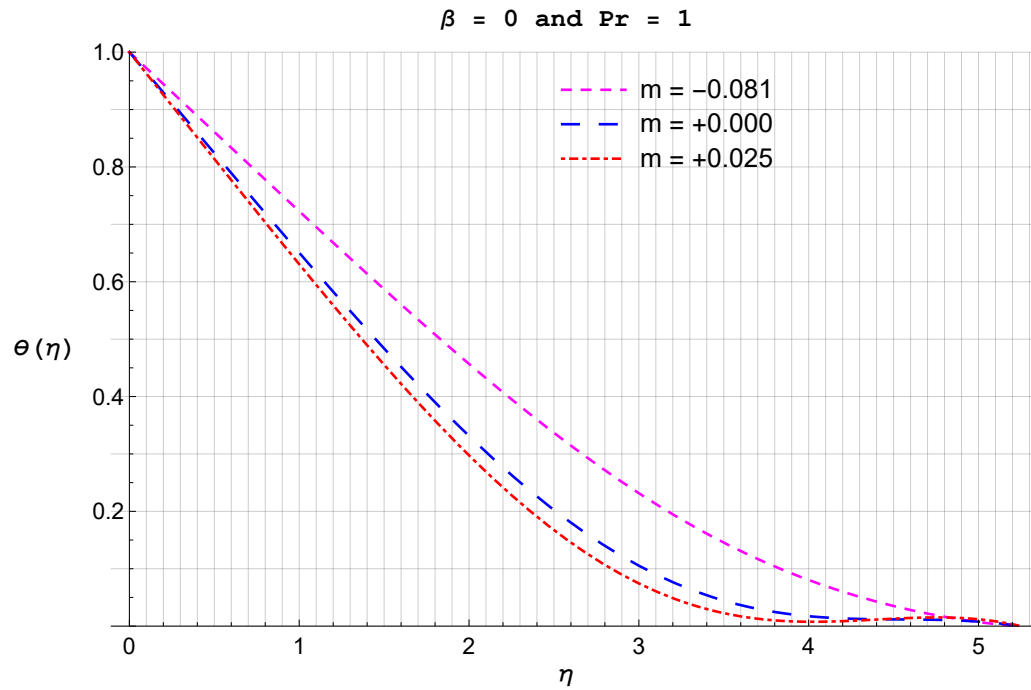


Figure 3: $\theta(\eta)$ for the Values m at $\beta = 0$ and $Pr = 1$

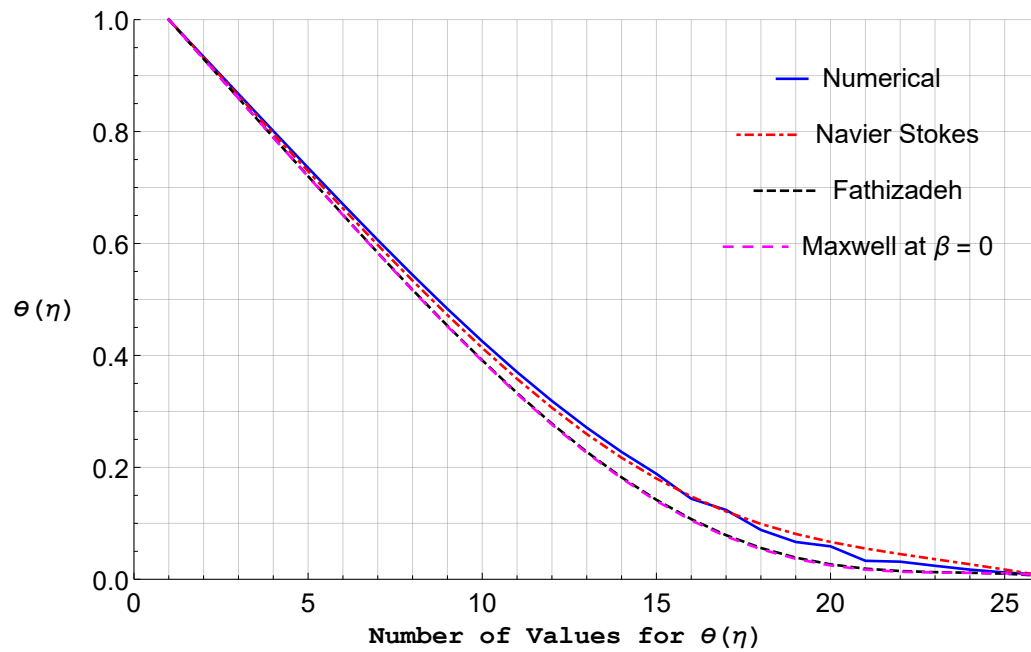


Figure 4: The Pictorial Comparison of $\theta(\eta)$ for the Values $m = 0$ When $\beta = 0$ and $Pr = 1$

Table 2: The Tabular Values of $f'(\eta)$ for the Figure 1

η	$f'(\eta)$		
	m		
	$\beta = 0$		
	0.000	-0.065	-0.120
0.0	0.000000	0.000000	0.000000
0.2	0.070328	0.037786	0.001397
0.4	0.140606	0.078154	0.007598
0.6	0.210705	0.121048	0.018608
0.8	0.280410	0.166368	0.034431
1.0	0.349425	0.213964	0.055056
1.2	0.417375	0.263621	0.080452
1.4	0.483811	0.315061	0.110550
1.6	0.548225	0.367935	0.145229
1.8	0.610057	0.421821	0.184304
2.0	0.668719	0.476226	0.227513
2.2	0.723611	0.530591	0.274500
2.4	0.774150	0.584303	0.324818
2.6	0.819799	0.636711	0.377919
2.8	0.860099	0.687143	0.433159
3.0	0.894707	0.734935	0.489814
3.2	0.923428	0.779465	0.547090
3.4	0.946255	0.820180	0.604156
3.6	0.963397	0.856640	0.660169
3.8	0.975307	0.888548	0.714316
4.0	0.982693	0.915783	0.765850
4.2	0.986519	0.938427	0.814126
4.4	0.987979	0.956766	0.858635
4.6	0.988443	0.971283	0.899021
4.8	0.989370	0.982614	0.935080
5.0	0.992164	0.991465	0.966726

Table 3: Absolute Error for $f'(\eta)$ of the Different Results

η	NM (1)	HPM					
		Fathizadeh & Rashidi [32]		Navier-Stokes		Maxwell $\beta = 0$	
		(2)	(1) – (2)	(3)	(1) – (3)	(4)	(1) – (4)
		$m = 0$	Error	$m = 0$	Error	$m = 0$	Error
0.0	0.000000	0.000000	0.000000	0.000000	0.000000	0.000000	0.000000
0.2	0.066407	0.070328	0.003920	0.067951	0.001543	0.070328	0.003920
0.4	0.132764	0.140606	0.007841	0.135847	0.003082	0.140606	0.007841
0.6	0.198937	0.210704	0.011767	0.203544	0.004606	0.210704	0.011767
0.8	0.264709	0.280410	0.015700	0.270803	0.006093	0.280410	0.015700
1.0	0.329780	0.349425	0.019645	0.337298	0.007518	0.349425	0.019645
1.2	0.393776	0.417374	0.023598	0.402616	0.008839	0.417374	0.023598
1.4	0.456261	0.483811	0.027549	0.466272	0.010010	0.483811	0.027549
1.6	0.516756	0.548224	0.031468	0.527725	0.010968	0.548224	0.031468
1.8	0.574758	0.610057	0.035299	0.586395	0.011636	0.610057	0.035299
2.0	0.629765	0.668718	0.038953	0.641694	0.011928	0.668718	0.038953
2.2	0.681310	0.723610	0.042300	0.693055	0.011744	0.723610	0.042300
2.4	0.728981	0.774149	0.045167	0.739966	0.010984	0.774149	0.045167
2.6	0.772455	0.819798	0.047343	0.782012	0.009557	0.819798	0.047343
2.8	0.811509	0.860099	0.048589	0.818912	0.007402	0.860099	0.048589
3.0	0.846044	0.894706	0.048662	0.850554	0.004509	0.894706	0.048662
3.2	0.876081	0.923427	0.047346	0.877026	0.000944	0.923427	0.047346
3.4	0.901761	0.946254	0.044493	0.898635	0.003126	0.946254	0.044493
3.6	0.923329	0.963396	0.040067	0.915908	0.007421	0.963396	0.040067
3.8	0.941118	0.975306	0.034188	0.929578	0.011540	0.975306	0.034188
4.0	0.955518	0.982692	0.027174	0.940539	0.014979	0.982692	0.027174
4.2	0.966957	0.986519	0.019562	0.949780	0.017177	0.986519	0.019562
4.4	0.975870	0.987978	0.012108	0.958285	0.017585	0.987978	0.012108
4.6	0.982683	0.988443	0.005759	0.966911	0.015772	0.988443	0.005759
4.8	0.987789	0.989370	0.001580	0.976249	0.011540	0.989370	0.001580
5.0	0.991541	0.992164	0.000622	0.986487	0.005054	0.992164	0.000622

Table 4: The Tabular Values of $\theta(\eta)$ for the Figure 3

η	$\theta(\eta)$		
	$\beta = 0.0$ and $Pr = 1$		
	m		
	-0.081	0.000	0.025
0.0	1.000000	1.000000	1.000000
0.2	0.944418	0.929672	0.925570
0.4	0.888850	0.859394	0.851201
0.6	0.833339	0.789295	0.777053
0.8	0.777957	0.719590	0.703385
1.0	0.722809	0.650575	0.630557
1.2	0.668039	0.582625	0.559021
1.4	0.613824	0.516189	0.489312
1.6	0.560382	0.451775	0.422034
1.8	0.507960	0.389943	0.357843
2.0	0.456840	0.331281	0.297428
2.2	0.407325	0.276389	0.241477
2.4	0.359731	0.225850	0.190651
2.6	0.314378	0.180201	0.145549
2.8	0.271576	0.139901	0.106661
3.0	0.231607	0.105293	0.074332
3.2	0.194711	0.076572	0.048719
3.4	0.161071	0.053745	0.029743
3.6	0.130794	0.036603	0.017055
3.8	0.103907	0.024693	0.010007
4.0	0.080354	0.017307	0.007630
4.2	0.059999	0.013480	0.008637
4.4	0.042655	0.012021	0.011448
4.6	0.028123	0.011556	0.014243
4.8	0.016264	0.010630	0.015064
5.0	0.007103	0.007835	0.011965

Table 5: Absolute Error for $\theta(\eta)$ of the Different Results

η	NM (1)	HPM					
		Fathizadeh & Rashidi [32]		Navier-Stokes [32]		Maxwell $\beta = 0$ [32]	
		(2)	(1) – (2)	(3)	(1) – (3)	(4)	(1) – (4)
		$m = 0$	Error	$m = 0$	Error	$m = 0$	Error
0.0	1.000000	1.000000	0.000000	1.000000	0.000000	1.000000	0.000000
0.2	0.933592	0.929826	0.003766	0.932044	0.001548	0.929672	0.003920
0.4	0.867235	0.859702	0.007533	0.864143	0.003092	0.859394	0.007841
0.6	0.801062	0.789758	0.011304	0.796441	0.004621	0.789295	0.011767
0.8	0.735290	0.720208	0.015082	0.729173	0.006117	0.719590	0.015700
1.0	0.670219	0.651348	0.018871	0.662666	0.007553	0.650575	0.019644
1.2	0.606223	0.583555	0.022667	0.597329	0.008894	0.582625	0.023598
1.4	0.543738	0.517277	0.026460	0.533644	0.010094	0.516189	0.027549
1.6	0.483243	0.453023	0.030219	0.472150	0.011093	0.451775	0.031468
1.8	0.425241	0.391350	0.033891	0.413418	0.011823	0.389943	0.035298
2.0	0.370234	0.332848	0.037386	0.358032	0.012202	0.331281	0.038953
2.2	0.318689	0.278111	0.040577	0.306551	0.012138	0.276389	0.042300
2.4	0.271018	0.227721	0.043296	0.259476	0.011542	0.225850	0.045168
2.6	0.227544	0.182208	0.045336	0.217212	0.010332	0.180201	0.047343
2.8	0.188490	0.142023	0.046467	0.180029	0.008461	0.139901	0.048589
3.0	0.143955	0.107501	0.036454	0.148027	0.004071	0.105293	0.038662
3.2	0.123918	0.078822	0.045095	0.121109	0.002809	0.076572	0.047346
3.4	0.088238	0.055982	0.032256	0.098964	0.010725	0.053745	0.034493
3.6	0.066670	0.038752	0.027917	0.081069	0.014399	0.036603	0.030067
3.8	0.058881	0.026666	0.032215	0.066706	0.007824	0.024693	0.034188
4.0	0.033042	0.018997	0.014045	0.055013	0.021970	0.017307	0.015735
4.2	0.031481	0.014772	0.016709	0.045053	0.013571	0.013480	0.018000
4.4	0.024129	0.012791	0.011338	0.035920	0.011791	0.012021	0.012108
4.6	0.017316	0.011691	0.005624	0.026858	0.009541	0.011556	0.005759
4.8	0.012210	0.010044	0.002165	0.017398	0.005187	0.010630	0.001580
5.0	0.008458	0.006500	0.001957	0.007485	0.000973	0.007835	0.000622

6 Conclusion

In this study is to compare and analyze the effects of the presence and absence of β , also the effects of m and Pr on the momentum and thermal boundary layer thicknesses. Both the fluid equations have been considered with the inclusion of pressure gradient parameter and solved them through an approximation technique Homotopy Perturbation Method (HPM) with an application of algorithms of Adams Method (AM) and Gear Method (GM), after applying similarity transformation which transforms these equations into an Ordinary Differential Equation (ODE). The obtained results have been compared for zero and non-zero Deborah number for the velocity and temperature profiles. Also validated the results, after comparing with the Fathizadeh and Rashidi previously published work. Those found to be in good agreement with the results obtained. At first the results have been compared with published results in [32], in case of Deborah number $\beta = 0$, pressure gradient $m = 0$, those found to be in good agreement. It can be observed that the velocity profile increases with an increase in pressure gradient m , consequently the momentum boundary layer thickness becomes thicker and thicker. Similarly, for energy in case of Deborah number $\beta = 0$, pressure gradient $m = 0$ and $Pr = 1$. As a whole energy profile decreases with an increase in pressure gradient m consequently, the thermal boundary layer thickness becomes thinner and thinner.

Acknowledgments

This research is being partially supported by the research grant under MOHE, FRGS project vote No.R.J 1300007809.4F354. The first author (ANK) is fully supported by Federal Urdu University of Arts, Sciences & Technology (FUUAST) Karachi, Pakistan under the Faculty Development Program (FDP) of Higher Education Commission (HEC) of Pakistan. Last but not least Dr. Muhammad Arif Hussain has given a great support in this research who is affiliated to Mohammad Ali Jinnah University, Karachi, Pakistan.

References

- [1] Chhabra, R. P. Non-newtonian fluids: an introduction. In *Rheology of complex fluids*. Springer. 3–34. 2010.
- [2] Málek, J. Introduction to non-newtonian fluid mechanics. 2012.
- [3] Hayat, T., Abbas, Z. and Sajid, M. Mhd stagnation-point flow of an upper-convected maxwell fluid over a stretching surface. *Chaos, Solitons & Fractals*. 2009. 39(2): 840–848.
- [4] Noor, N. F. M. Analysis for mhd flow of a maxwell fluid past a vertical stretching sheet in the presence of thermophoresis and chemical reaction. *World Acad. Sci., Eng. Technol*. 2012. 64: 1019–1023.
- [5] Motsa, S., Khan, Y. and Shateyi, S. A new numerical solution of maxwell fluid over a shrinking sheet in the region of a stagnation point. *Mathematical Problems in Engineering*. 2012. 2012.

- [6] Omowaye, A. and Animasaun, I. Upper-convected maxwell fluid flow with variable thermo-physical properties over a melting surface situated in hot environment subject to thermal stratification. *J. Appl. Fluid Mech.* 2016. 9(4): 1777–1790.
- [7] Maxwell, J. C. On the dynamical theory of gases. *Philosophical transactions of the Royal Society of London.* 1867. 157: 49–88.
- [8] Shateyi, S. A new numerical approach to mhd flow of a maxwell fluid past a vertical stretching sheet in the presence of thermophoresis and chemical reaction. *Boundary Value Problems.* 2013. 2013(1): 1–14.
- [9] Abbas, Z., Sajid, M. and Hayat, T. Mhd boundary-layer flow of an upper-convected maxwell fluid in a porous channel. *Theoretical and Computational Fluid Dynamics.* 2006. 20(4): 229–238.
- [10] Hayat, T., Mustafa, M. and Mesloub, S. Mixed convection boundary layer flow over a stretching surface filled with a maxwell fluid in presence of solet and dufour effects. *Zeitschrift für Naturforschung A.* 2010. 65(5): 401–410.
- [11] Jafar, K., Ishak, A. and Nazar, R. Mhd stagnation-point flow over a nonlinearly stretching/shrinking sheet. *Journal of Aerospace Engineering.* 2011. 26(4): 829–834.
- [12] Tilley, B. and Weidman, P. Oblique two-fluid stagnation-point flow. *European Journal of Mechanics-B/Fluids.* 1998. 17(2): 205–217.
- [13] Clancy, L. *Aerodynamics*, section 3.3, 3.5, 3.12. 1975.
- [14] Abbasbandy, S. Application of he’s homotopy perturbation method for laplace transform. *Chaos, Solitons & Fractals.* 2006. 30(5): 1206–1212.
- [15] Beléndez, A., Hernandez, A., Beléndez, T., Fernández, E., Alvarez, M. and Neipp, C. Application of he’s homotopy perturbation method to the duffing-harmonic oscillator. *International Journal of Nonlinear Sciences and Numerical Simulation.* 2007. 8(1): 79–88.
- [16] Cai, X., Wu, W. and Li, M. Approximate period solution for a kind of nonlinear oscillator by he’s perturbation method. *Int. J. Nonlinear Sci. Numer. Simulation.* 2006. 7(1): 109–112.
- [17] Cveticanin, L. Homotopy–perturbation method for pure nonlinear differential equation. *Chaos, Solitons & Fractals.* 2006. 30(5): 1221–1230.
- [18] Ghori, Q., Ahmed, M. and Siddiqui, A. Application of homotopy perturbation method to squeezing flow of a newtonian fluid. *International Journal of Nonlinear Sciences and Numerical Simulation.* 2007. 8(2): 179–184.
- [19] Ji-Huan, H. Approximate solution of nonlinear differential equations with convolution product nonlinearities. *Computer Methods in Applied Mechanics and Engineering.* 1998. 167(1): 69–73.

- [20] Ji-Huan, H. Homotopy perturbation technique. *Computer methods in applied mechanics and engineering*. 1999. 178(3): 257–262.
- [21] Eric Weisstein, W. Adams Method. URL FromMathWorld--AWolframWebResource.<http://mathworld.wolfram.com/AdamsMethod.html>.
- [22] Wolfgang, C. Gear Method. 2007. URL UniversityofCalifornia--SanDiego,<http://renaissance.ucsd.edu/chapters/chap11.pdf>.
- [23] Matthew, B., Olyvia, D., Viral, P., Joel, S. and Eric Van, B. Adams and Gear methods for Solving ODEs with Mathematica. 2007. URL https://controls.engin.umich.edu/wiki/index.php/Solving_ODEs_with_Mathematica.
- [24] Hayat, T., Shehzad, S. and Alsaedi, A. Study on three-dimensional flow of maxwell fluid over a stretching surface with convective boundary conditions. *International Journal of Physical Sciences*. 2012. 7(5): 761–768.
- [25] Bhattacharyya, K., Hayat, T. and Gorla, R. S. R. Heat transfer in the boundary layer flow of maxwell fluid over a permeable shrinking sheet. *Thermal Energy and Power Engineering*. 2013. 2(3): 72–78.
- [26] Cebeci, T. and Bradshaw, P. *Physical and Computational Aspects of Convective Heat Transfer*. New York: Springer-Verlag. 1988.
- [27] Rebay, M. and Padet, J. Parametric study of unsteady forced convection with pressure gradient. *International journal of engineering science*. 2005. 43(8): 655–667.
- [28] Shagaiya, Y. and Daniel, S. Presence of Pressure Gradient on Laminar Boundary Layer over a Permeable Surface with Convective Boundary Condition. *American Journal of Heat and Mass Transfer*. 2015. 2(1): 1–14.
- [29] Kakaç, S. and Yener, Y. *Convective heat transfer*. Middle East Technical University. 1980.
- [30] Eosboee, M. R., Pourmahmoud, N., Mirzaie, I., Khameneh, P. M., Majidyfar, S. and Ganji, D. Analytical and numerical analysis of mhd boundary layer flow of an incompressible upper-convected maxwell fluid. *International Journal of Engineering Science and Technology*. 2010. 2(12): 6909–6917.
- [31] Abbas, Z., Wang, Y., Hayat, T. and Oberlack, M. Mixed convection in the stagnation-point flow of a maxwell fluid towards a vertical stretching surface. *Nonlinear Analysis: Real World Applications*. 2010. 11(4): 3218–3228.
- [32] Fathizadeh, M. and Rashidi, F. Boundary layer convective heat transfer with pressure gradient using Homotopy Perturbation Method (HPM) over a flat plate. *Chaos, Solitons & Fractals*. 2009. 42(4): 2413–2419.